

Seeing the Future, Perceiving the Future: A Unified Driving World Model for Future Generation and Perception

Dingkang Liang^{*1}, Dingyuan Zhang^{*1}, Xin Zhou^{*1}, Sifan Tu¹,
Tianrui Feng¹, Xiaofan Li², Yumeng Zhang², Mingyang Du¹, Xiao Tan², Xiang Bai^{†1}

¹Huazhong University of Science and Technology, ²Baidu Inc., China
{dkliang, dyzhang233, xzhou03}@hust.edu.cn

Abstract

We present *UniFuture*, a simple yet effective driving world model that seamlessly integrates future scene generation and perception within a single framework. Unlike existing models focusing solely on pixel-level future prediction or geometric reasoning, our approach jointly models future appearance (i.e., RGB image) and geometry (i.e., depth), ensuring coherent predictions. Specifically, during the training, we first introduce a *Dual-Latent Sharing* scheme, which transfers image and depth sequence in a shared latent space, allowing both modalities to benefit from shared feature learning. Additionally, we propose a *Multi-scale Latent Interaction* mechanism, which facilitates bidirectional refinement between image and depth features at multiple spatial scales, effectively enhancing geometry consistency and perceptual alignment. During testing, our *UniFuture* can easily predict high-consistency future image-depth pairs by only using the current image as input. Extensive experiments on the nuScenes dataset demonstrate that *UniFuture* outperforms specialized models on future generation and perception tasks, highlighting the advantages of a unified, structurally-aware world model. The project page is at <https://github.com/dk-liang/UniFuture>.

1. Introduction

Driving World Models (DWMs) [8, 22, 32, 33, 39, 48] play a vital role in self-driving, allowing the ego-vehicle to predict future scene evolution based on current or history scene information. These models enable self-driving systems to anticipate potential hazards, simulate different scenarios, and make informed decisions. Moreover, DWMs can expand training data, especially for rare or safety-critical situations, and support the construction of end-to-end reinforce-

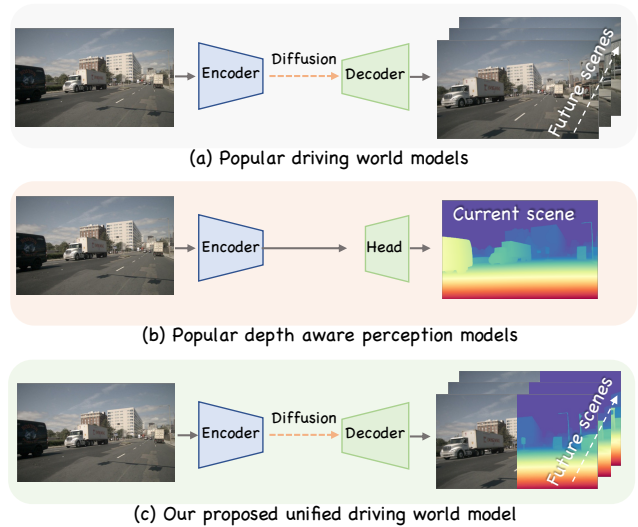


Figure 1. (a) Popular driving world models focus only on low-level visual representations (i.e., RGB images). (b) Depth estimation models provide high-level geometric information but lack future scene evolution. (c) Our **UniFuture** unifies future generation and perception in a simple yet effective manner.

ment learning models by providing realistic simulated environments for training.

Recent advancements in DWMs have leveraged powerful generative models, especially large-scale pre-trained diffusion models, to achieve fine-grained future scene generation. In particular, the popular DWMs [8, 23, 35, 36, 41] predominantly focus on RGB image synthesis, aiming to generate visually realistic representations of upcoming driving scenes, as shown in Fig. 1(a). However, despite achieved advances, these DWMs predict low-level visual representations (e.g., RGB pixels) but overlook geometry information, particularly depth, which is essential for autonomous driving. Future depth estimation is crucial for understanding the layout of a scene, enabling accurate object position-

^{*}Equal contribution. [†]Corresponding author.

ing, obstacle avoidance, and safe path planning. Without depth-aware predictions, DWMs struggle to provide meaningful spatial reasoning, leading to challenges in handling occlusions, estimating distances, and understanding scene dynamics in a geometrically consistent manner.

On the other hand, depth-aware perception models [6, 25, 40, 42] focus on extracting structural information to support downstream tasks like motion planning. While these models provide a high-level geometric understanding of the scene, they lack explicit future prediction capabilities, as most depth estimation approaches rely on present and past frames without modeling how the scene structure will evolve in the future, as shown in Fig. 1(b). These limitations raise an interesting and practical topic: *can we develop a unified driving world model that integrates future prediction with perception?*

To achieve this goal, we propose **UniFuture**, a unified world model that enables simultaneous forecasting of scene evolution and high-level geometric understanding, as shown in Fig. 1(c). Specifically, although most diffusion models are pre-training on the appearance (image) space, we reveal that image and geometric (depth) information are heterogeneous representations of the same scene, making bidirectional transformation between them both natural and beneficial. To facilitate this, we introduce a simple Dual-Latent Sharing (DLS) scheme, which maps image and depth into a shared latent space. Instead of training a separate Auto-Encoder (AE) for depth, we directly leverage the pre-trained image AE, sharing its encoder and decoder across both modalities. This eliminates additional AE pre-training and ensures effective cross-domain feature alignment, enabling direct transformations between image and depth using a simple neural network.

Building on the aligned representation, we further propose a Multi-scale Latent Interaction (MLI) mechanism to enable cross-modal refinement. Embedded within the multi-scale UNet structure, MLI facilitates bidirectional interaction between image and depth representations. During future predictions, the image latent is first converted into an initial depth latent and then iteratively refined across multiple scales. To enhance structural consistency, the depth latent is injected back into the image latent space and propagated further into the depth stream, encouraging geometric priors in image predictions while maintaining visual coherence for depth estimation. This mutual interaction leads to a structured and geometry-aware future scene generation, seamlessly integrating low-level pixel synthesis with high-level spatial reasoning.

Our unified world model offers several key advantages over conventional pipelines. First, by unifying future generation and perception, image synthesis benefits from depth priors, enhancing structural coherence, while depth estimation leverages rich appearance priors, improving geometric

consistency. Second, the shared latent space enables seamless interaction between image and depth modalities, leading to improved cross-modal alignment and more reliable predictions. Besides, since the model can jointly predict both future visual scenes and structured high-level information, it becomes a potential model for automated annotation, e.g., using an image as input can generate highly consistent future image-depth pairs.

Extensive experiments on the nuScenes dataset show that **UniFuture** achieves state-of-the-art performance in both generation and perception. Compared to our baseline Vista [8], we reduce FID by 23.9% and improve FVD under the same resolution, demonstrating the superior generation ability of our method. Additionally, for the future perception task, we outperform Marigold [20] (also trained with future supervision) by a large margin.

The main contributions are summarized as follows: **1)** We propose **UniFuture**, a unified world model that seamlessly integrates future scene generation and perception, allowing appearance and geometry to be jointly modeled within a single framework. This synergy enables structured, coherent future predictions while enhancing depth-aware reasoning. **2)** We introduce a simple Dual-Latent Sharing (DLS) scheme and the Multi-scale Latent Interaction (MLI) mechanism to unify image and depth representations in a shared latent space and enable bidirectional multi-scale refinement. **3)** Despite its simplicity, we still achieve impressive performance in both tasks, offering a viable alternative to specialized future generation and perception models.

2. Related Work

2.1. World Models in Autonomous Driving

World models predict scene evolution based on current observations [10, 12] and have become a key focus in autonomous driving. Many approaches [21, 23, 24, 36] excel in forecasting 2D visual representations, demonstrating strong dynamic modeling capabilities.

Most methods rely on generative techniques like autoregressive transformers [5, 15] and diffusion models [11, 19, 37] for future video prediction. Specifically, GAIA-1 [15] formulates world modeling as a sequence task using an autoregressive transformer, while ADriver-I [18] integrates multi-modal LLMs and diffusion for control and frame generation. DriveDreamer [33] enforces structured traffic constraints in diffusion-based prediction, with DriveDreamer-2 [47] further incorporating LLMs for customizable video generation. Drive-WM [34] enhances multi-view consistency via view factorization, and GenAD [41] introduces large-scale video datasets to improve zero-shot generalization. Based on GenAD, Vista [8] enhances dynamics and preserves structural details with two extra loss functions, achieving high-resolution, high-fidelity, and long-

term scene evolution prediction. Subsequent works have made significant advancements in prediction duration [11, 17] and the integration of prediction with planning [5, 35].

Despite advancements, these world models only focus on low-level visual representations and overlook the geometry information, which hinders the ability of spatial reasoning. Instead, the proposed **UniFuture** integrates visual information with geometry features seamlessly, empowering the geometry-aware reasoning ability of the world model.

A concurrent work. We note a recent work, GEM [13], also proposes a unified framework for future image and depth prediction, with its publication occurring concurrently with the preparation of this manuscript. GEM concatenates the noisy image and depth latent, jointly denoising them in a UNet to enforce implicit consistency. However, this approach balances image and depth within the same denoising process, potentially limiting the effectiveness of pre-trained image models due to modality differences. In contrast, our method explicitly decouples image and depth spaces while enabling cross-modal interaction. This preserves the generative capacity of image pre-training while allowing depth priors to refine image synthesis and image appearance to enhance depth estimation, resulting in structurally and geometrically consistent predictions.

2.2. Monocular Depth Estimation

Monocular depth estimation, which aims to recover the geometry information from a single image or video, has gained significant attention in autonomous driving research [26]. Conventional works [1, 7, 9, 30, 45, 46] leverage multi-scale feature fusion to combine global and local depth information, achieving remarkable performance within specific domains. However, these methods have limited generalization ability due to the insufficient data scale and diversity. Some efforts address this by scaling data. MiDaS [27] and ZoeDepth [2] leverage multi-dataset joint training to enhance generalization, while DepthAnything [42, 43] explores large-scale unlabeled and synthetic data to improve detail modeling in complex scenes. Another progressing direction tries to incorporate rich priors of generative models (e.g., diffusion models) trained on vast amounts of wild images. Marigold [20] pioneers the use of Stable Diffusion [29] for affine-invariant depth estimation, followed by Lotus [14], which refines denoising schedules for better adaptation. DepthMaster [31] introduces a feature enhancement module to balance generative and discriminative representations, while DepthCrafter [16] extends this framework to open-world videos for consistent long-sequence depth estimation.

While existing depth estimation methods focus on perceiving the current or past environment, our approach integrates future depth estimation with the world model. This synergy leverages the world model’s reasoning capabilities

for high-quality depth prediction while using precise geometric cues to enhance dynamic scene modeling.

3. Preliminary

Stable Video Diffusion (SVD) [3] is a latent diffusion model designed for a high-resolution image-to-video generation. It employs a VAE to encode the input video into a latent space, followed by the diffusion process. It generates videos by denoising several frames using a video denoising UNet, which incorporates Conv3D and temporal attention layers between the original spatial layers.

Due to its strong video generation capabilities, SVD has become a core component in many Driving World Models (DWMs) [38, 41, 44]. A quintessence is Vista [8], our baseline method, which extends SVD for predictive driving scene synthesis, with additional constraints to improve the realism and consistency of generated driving videos (for further details, please refer to the original paper [8]). However, Vista and other SVD-based methods remain limited to future RGB-only generation, neglecting essential perception information, which is critical for autonomous driving.

4. Method

This paper proposes a unified world model, **UniFuture**, seamlessly integrating future scene generation with depth-aware perception. Built upon an SVD-based framework [8], our approach relieves the inherent gap between appearance (image) and geometry (depth) through two key components: 1) A very simple Dual-Latent Sharing (DLS) scheme, which maps both modalities into a shared latent space, enabling effective transformation between them without additional pre-training, and 2) Multi-scale Latent Interaction (MLI) mechanism, a feedback-driven mechanism that facilitates multi-scale bidirectional refinement between image and depth representations. These components ensure that both pixel-level synthesis and spatial reasoning evolve coherently.

During training (Fig. 2), **UniFuture** takes an image-depth pair sequence with M frames as input and maps them into a shared latent space. The image latent feature follows the classic denoising process*, while the depth latent feature is optimized using its corresponding loss.

During inference (Fig. 3), given a single input image without depth, we will concatenate $(M - 1) \times$ noise embeddings and then predict the future image-depth pairs with $(M - 1) \times$ frames, generating temporally and geometrically consistent future frames.

4.1. Dual-Latent Sharing Scheme

An image and its corresponding depth map describe the same underlying scene. Even though the latent encoder/decoder is pre-trained on RGB images, we argue that it can be

*The first frame is without noise as a condition frame.

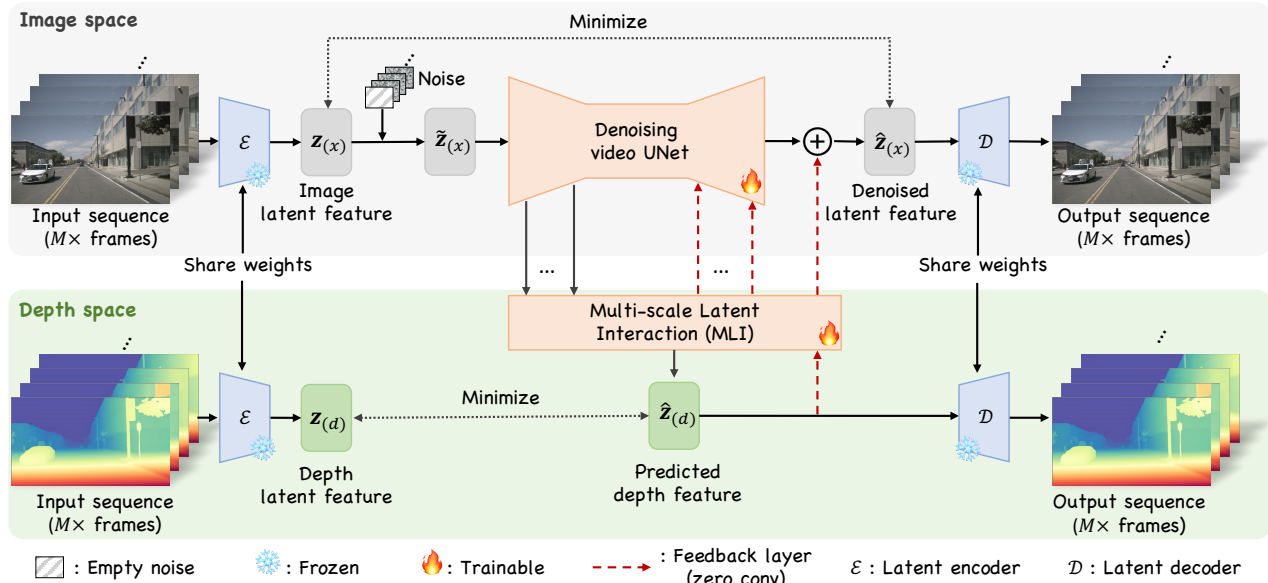


Figure 2. The training pipeline of **UniFuture**. The Dual-Latent Sharing (DLS) scheme unifies image and depth sequence in a shared latent space without additional pre-training. The image latent undergoes a denoising process, while the depth latent is explicitly predicted. The Multi-scale Latent Interaction (MLI) mechanism enables bidirectional refinement, enhancing consistency in future prediction.

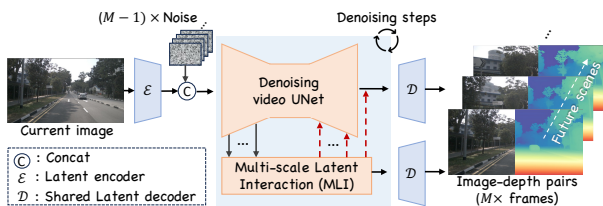


Figure 3. The inference pipeline of **UniFuture**, which takes a single image as input and predicts future image-depth pairs. The encoded image latent is concatenated with noise and denoised through the video UNet, followed by a shared decoder that predicts both future images and depth map sequences.

adapted to a unified latent space for both image and depth representations. To achieve this, we introduce an extremely simple yet effective Dual-Latent Sharing (DLS) scheme to unify their representations within a shared latent space, naturally enabling bidirectional feature interaction.

As shown in Fig. 2, given an image sequence x and its corresponding depth maps d , we process both through a shared pre-trained latent encoder \mathcal{E} , obtaining their respective latent representations $z(x)$ and $z(d)$. The image latent feature $z(x)$ undergoes the standard diffusion process, i.e., from $z(x)$ to $\hat{z}(x)$. Meanwhile, the depth latent feature $\hat{z}(d)$ is predicted through the following Multi-scale Latent Interaction (MLI) mechanism, ensuring geometry alignment between both modalities. Finally, both latent features are reconstructed back to pixel space using the shared latent decoder \mathcal{D} . By unifying image and depth within a shared latent space, DLS eliminates the need for additional depth autoencoder pre-training while ensuring seam-

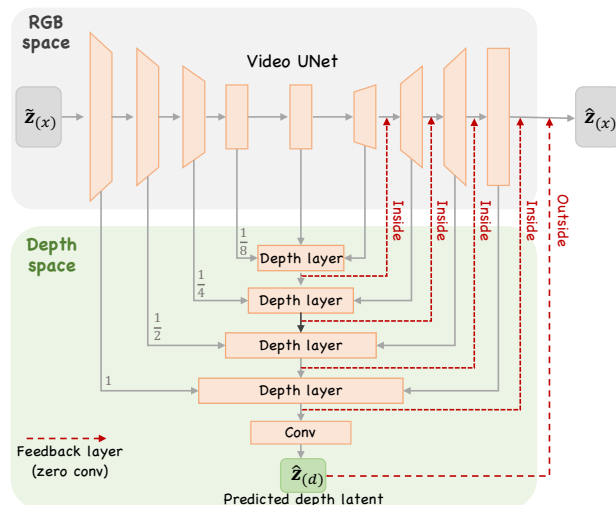


Figure 4. The details of our proposed Multi-scale Latent Interaction (MLI) mechanism.

less cross-modal interaction, forming the geometry-aware future prediction.

4.2. Multi-scale Latent Interaction Mechanism

To facilitate bidirectional interaction between image and depth representations, we propose the Multi-scale Latent Interaction (MLI) mechanism to incorporate explicit interaction between image and depth space. As shown in Fig. 4, MLI contains three parts: a series of depth layers to achieve feature fusion, multi-scale inside feedback, and fine-grained outside feedback, ensuring geometry consistency between image and depth.

Depth layer. To progressively transform the image latent feature into the depth space and establish a foundation for cross-modal interaction, we introduce a hierarchical feature fusion strategy through a series of depth layers. Specifically, as shown in Fig. 4, four scales $\{1, \frac{1}{2}, \frac{1}{4}, \frac{1}{8}\}$ of the UNet architecture is incorporated. Each depth layer fuses features from the corresponding UNet encoder and decoder scales with the output of the preceding depth layer. This fusion involves concatenating the encoder and decoder features, reducing dimensionality with a convolution, and then concatenating the previous depth layer’s output, followed by another dimensionality-reducing convolution. Finally, a bilinear upsample is used to produce the current depth layer’s output (the depth layer at scale 1 without upsampling).

Inside feedback. While image and depth share the same latent encoder, their inherent differences hinder direct feature interaction. To ensure the model learns stably at the beginning of training, we apply a zero-initialized convolution to process the intermediate depth latent feature \mathbf{X} . As shown in the red lines in Fig. 4, inside feedback comes from middle depth latent to the output of the UNet stages. The feedback depth response can be simply formulated as:

$$\mathbf{Y} = \text{ZeroConv}(\mathbf{X}), \quad (1)$$

where \mathbf{Y} will be added to the corresponding UNet stage. As the depth and image spaces have an inherent gap, we gradually learn the optimal transformation between the two spaces by initializing the convolution weights to zero, ensuring a smooth adaptation process.

Outside feedback. In addition to the multi-scale inside feedback, we further introduce an outside feedback mechanism to align the final predicted image and depth latent features. The predicted depth latent $\hat{z}_{(d)}$, derived by the output of the last depth layer via a convolution, is also injected into the denoised image latent as in Eq. 1.

A denoising step encompasses the UNet’s processing from input to generating the denoised latent feature $\hat{z}_{(x)}$ after outside feedback. By incorporating the components above, the MLI achieves the bidirectional interaction between the future prediction and perception, allowing the model to simultaneously generate high-consistency future image-depth pairs.

4.3. Training Objectives

Our training objectives include constraints in image and depth spaces. Specifically, at the latent level, we minimize the distance between the denoised image latent $\hat{z}_{(x)}$ and the input image latent features $z_{(x)}$ using a loss function $\mathcal{L}_{(x)}$ comprising MSE loss, dynamic enhancement loss, and structural preserving loss as in Vista [8]. A similar loss formulation $\mathcal{L}_{(d)}$ is also applied to the depth latent representations. For improved perception and finer details, we further employ the scale- and shift-invariant loss \mathcal{L}_{SSI}

between predicted and input depth maps, following Depth Anything [27]. The overall loss is a weighted sum:

$$\mathcal{L} = \mathcal{L}_{(x)} + \mathcal{L}_{(d)} + \lambda \cdot \mathcal{L}_{SSI}, \quad (2)$$

where λ balances the losses.

4.4. Inference Phase

Unlike previous approaches that focus solely on future prediction or depth estimation, our **UniFuture** leverages a single frame to generate temporally and geometrically consistent future image-depth pairs, as illustrated in Fig. 3. Specifically, we encode the input image into a latent representation, concatenate it with $(M - 1) \times$ Gaussian noise maps, and refine it through denoising iterations using a Multi-scale Latent Interaction (MLI)-enhanced UNet. After executing the schedule of multiple denoising steps, the final image and depth latent are decoded back into pixel space using the shared pre-trained AE decoder, producing high-consistency image-depth pairs. This ensures our model maintains perceptual realism and structural coherence across future predictions.

5. Experiments

5.1. Dataset and Evaluation Metric

We conduct experiments on the nuScenes dataset [4], a large-scale autonomous driving benchmark that provides multi-modal sensor data, including RGB images, LiDAR point clouds, and scene annotations. It contains 1,000 driving sequences collected in diverse urban environments. Following Vista [8], we use the front-camera RGB frames as the main training data. Since there are no pixel-wise dense depth labels for nuScenes [4], we adopt off-the-shelf DepthAnythingV2 [43] as the pseudo depth label generator, considering its strong generalization capabilities across various types of images.

Evaluation metric. For the generation task, we evaluate the quality and realism of generated frames using Fréchet Inception Distance (FID) and Fréchet Video Distance (FVD), which measure the distributional similarity between generated and real images/videos. Lower FID and FVD scores indicate better generation quality. For the depth estimation task, we use Absolute Relative Error (AbsRel) to quantify relative depth differences and threshold accuracy (δ) to measure the proportion of accurate predictions within a specified relative error. Higher δ values and lower AbsRel values indicate better depth estimation performance. It should be noted that to evaluate the consistency between the predicted future depth and the future scene. We utilize DepthAnythingV2 [43] to process the predicted future scene as pseudo-depth labels when computing the aforementioned depth metrics unless otherwise specified.

Table 1. Comparison of our method with specialized generation and perception models. \star marks our baseline method, which is fine-tuned under the same resolution and iteration constraints using the official pre-trained weight of Vista [8]. Our method predicts depth up to 25 future frames, while Marigold [20] supports only single-frame depth estimation. To enable a reasonable comparison, we train Marigold with next-frame supervision using the 1st and 12th future frames. \blacklozenge marks these settings.

Method	Reference	Resolution	Generation		Perception			
			FID \downarrow	FVD \downarrow	AbsRel \downarrow	$\delta_1 \uparrow$	$\delta_2 \uparrow$	$\delta_3 \uparrow$
Only future perception								
Marigold (0-th frame) [20]	CVPR 24	320×576			20.4	80.3	93.1	96.5
Marigold (1-st frame) \blacklozenge [20]	CVPR 24	320×576	Unsupported		21.9	77.7	91.2	95.6
Marigold (12-th frame) \blacklozenge [20]	CVPR 24	320×576			39.0	65.8	81.9	89.7
Only future generation								
DriveGAN [21]	CVPR 21	256×256	73.4	502.3				
DriveDreamer [33]	ECCV 24	128×192	52.6	452.0				
WoVoGen [24]	ECCV 24	256×448	27.6	417.7				
DrivingDiffusion [23]	ECCV 24	512×512	15.8	332.0				
GenAD [41]	CVPR 24	256×448	15.4	184.0		Unsupported		
Panacea [36]	CVPR 24	256×512	17.0	139.0				
Drive-WM [35]	CVPR 24	192×384	15.2	122.7				
Vista \star [8] (baseline)	NeurIPS 24	320×576	15.5	101.5				
Unify future perception and generation								
UniFuture (ours)	-	320×576	11.8	99.9	8.936	91.4	97.6	98.9

5.2. Implementation details

Our model is trained with a batch size of 1 on $8 \times$ NVIDIA H20 GPUs. We use the AdamW optimizer with a learning rate of 5×10^{-5} , and the training process runs for 8K iterations to ensure convergence. Besides, following Vista [8], we use the Exponential Moving Average (EMA) strategy to make training stable and drop out each activated action mode with a ratio of 15% to allow classifier-free guidance. To optimize memory usage, we adopt the DeepSpeed ZeRO-2 [28] strategy, which effectively reduces memory overhead. We set the length of video $M = 25$, and the loss balance weight $\lambda = 0.5$.

5.3. Main Results

We evaluate **UniFuture** on both future generation and future perception tasks. Our goal is to explore the potential of unifying these two tasks within a single framework. We select Vista [8], a widely used world model in autonomous driving, as our baseline. As shown in Tab. 1, our method achieves highly competitive performance in both future generation and perception tasks. The results lead to the following key observations.

For the future generation task, compared to the baseline Vista [8], our **UniFuture** achieves a significant 3.7-point reduction in FID (from 15.5 to 11.8) while obtaining a highly competitive FVD score under the same resolution. These improvements indicate that incorporating future perception enhances structure preservation and overall visual coherence in generated future frames. Notably, existing state-of-the-art world models [8, 23, 36] focus solely on future low-level pixel-space synthesis, leading to limited

Table 2. Zero-shot results on the Waymo dataset.

Method	Generation		Perception			
	FID \downarrow	FVD \downarrow	AbsRel \downarrow	$\delta_1 \uparrow$	$\delta_2 \uparrow$	$\delta_3 \uparrow$
Vista [8] (baseline)	23.8	238.4		Unsupported		
UniFuture (ours)	16.3	227.6	9.517	89.3	97.0	98.7

scene understanding (also see Fig. 5). By contrast, our approach integrates geometric priors into the generative process, improving consistency in predicted frames.

For the future perception task, **UniFuture** achieves state-of-the-art depth estimation performance, significantly outperforming Marigold [20]. It achieves the lowest AbsRel error (8.936) and the highest threshold accuracy ($\delta_1 = 91.4$, $\delta_2 = 97.6$, $\delta_3 = 98.9$), demonstrating superior depth estimation quality. In contrast, Marigold, which is explicitly designed for monocular depth estimation, lacks future scene modeling capabilities and is limited to single-frame predictions. Even when adapted for next-frame supervision, its performance degrades at longer horizons (AbsRel 39.0 at the 12th frame), highlighting its difficulty in long-term depth forecasting. By leveraging the Dual-Latent Sharing and Multi-scale Latent Interaction, **UniFuture** seamlessly integrates future scene understanding into depth prediction, leading to better geometrically consistent (also see Fig. 5).

5.4. Zero-Shot Comparison

To evaluate generalization ability, we test **UniFuture** on the Waymo dataset without fine-tuning. As shown in Tab. 2, our method outperforms Vista [8] in future generation, achieving a 7.5-point lower FID (16.3 vs. 23.8) and improved

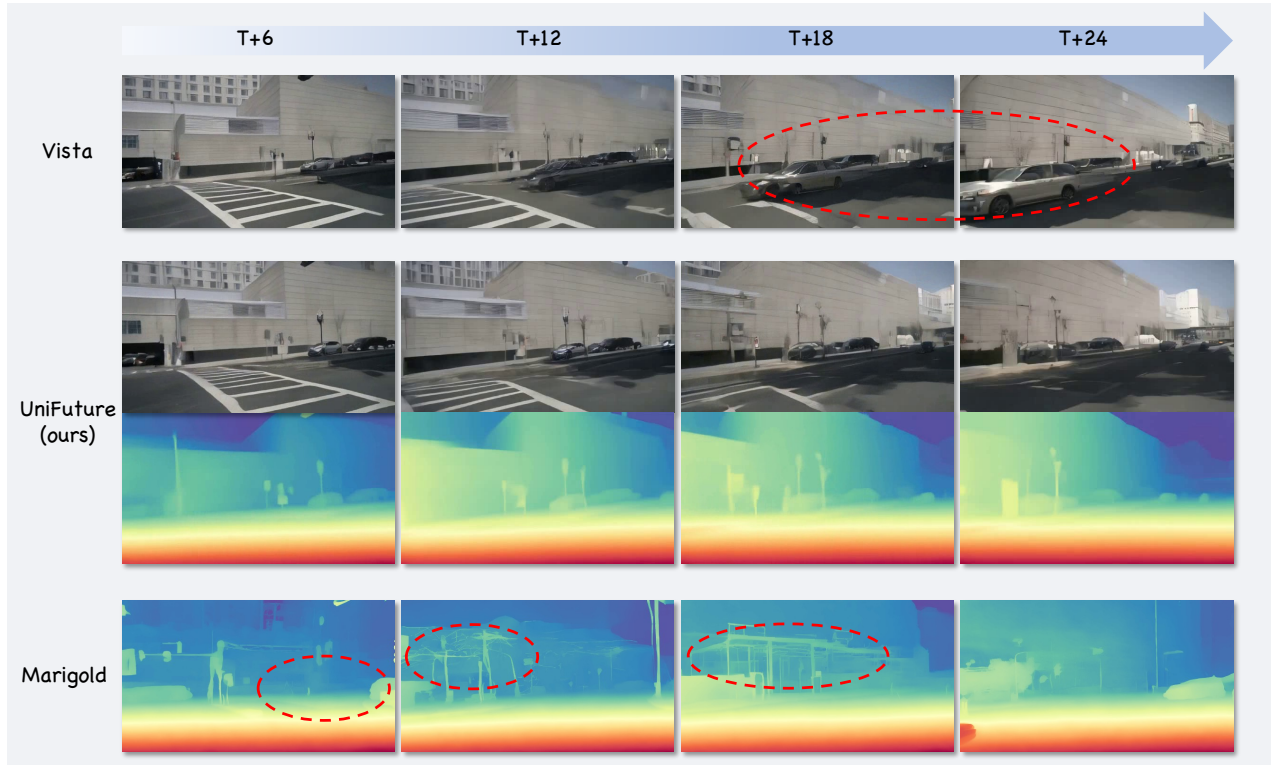


Figure 5. Qualitative comparisons between different models. The existing world model (Vista [8]) lacks depth awareness, leading to inaccurate scene understanding. Depth estimation models (Marigold [20]) fail to predict future depth, limiting their ability to capture scene evolution. In contrast, our **UniFuture** delivers more coherent future predictions, enhancing both generation and perception tasks.

Table 3. The effectiveness of optimized paradigms.

Setting	Image	Depth	Generation		Perception			
			FID ↓	FVD ↓	AbsRel ↓	δ_1 ↑	δ_2 ↑	δ_3 ↑
Image-only	✓	-	15.5	101.5	Unsupported			
Depth-only	-	✓	271.0	3143.2	24.196	62.0	84.5	92.4
Detach-grad	✓	✓	11.2	104.9	12.351	85.2	95.2	97.8
Joint training	✓	✓	11.8	99.9	8.936	91.4	97.6	98.9

FVD, demonstrating stronger visual coherence in unseen domains. Additionally, while Vista lacks perception capabilities, our method provides accurate zero-shot depth estimation (AbsRel = 9.517, $\delta_1 = 89.3$), benefiting from its cross-modal interaction and geometry-aware modeling. These results highlight the potential generalization ability of our unified approach, enabling better future scene generation and perception under domain shifts.

5.5. Ablation Study

This section discusses the key designs of our method, including the different optimized paradigms, the detailed analysis of the Dual-Latent Sharing (DLS) scheme, and the Multi-scale Latent Interaction (MLI) mechanism.

The impact of different optimize paradigms. We first study the impact of different optimization paradigms, in-

Table 4. The effectiveness of different decoders for depth space.

Decoder	Generation		Perception			
	FID ↓	FVD ↓	AbsRel ↓	δ_1 ↑	δ_2 ↑	δ_3 ↑
Conventional decoder	15.6	121.1	11.874	86.4	95.9	98.1
Our DLS	11.8	99.9	8.936	91.4	97.6	98.9

cluding image-only training, depth-only training, separate optimization with detached gradients, and our joint training paradigm. As shown in Tab. 3, we can make the following observations: 1) Training only the image space achieves reasonable generation quality but lacks depth perception capabilities, while training only the depth space results in sub-par depth estimation and fails to generate reasonable future scenes. 2) Separate optimization, i.e., detaching gradients between image and depth spaces, provides limited improvements over single-task training. While it helps depth estimation, it degrades generation quality (higher FVD) due to the lack of geometry consistency reinforcement. 3) Our joint training, which allows gradient flow between image and depth spaces, consistently improves both future generation (mainly for FVD) and perception, leading to the best performance across all metrics.

The effectiveness of the DLS scheme. We then evaluate the effectiveness of the Dual-Latent Sharing (DLS)

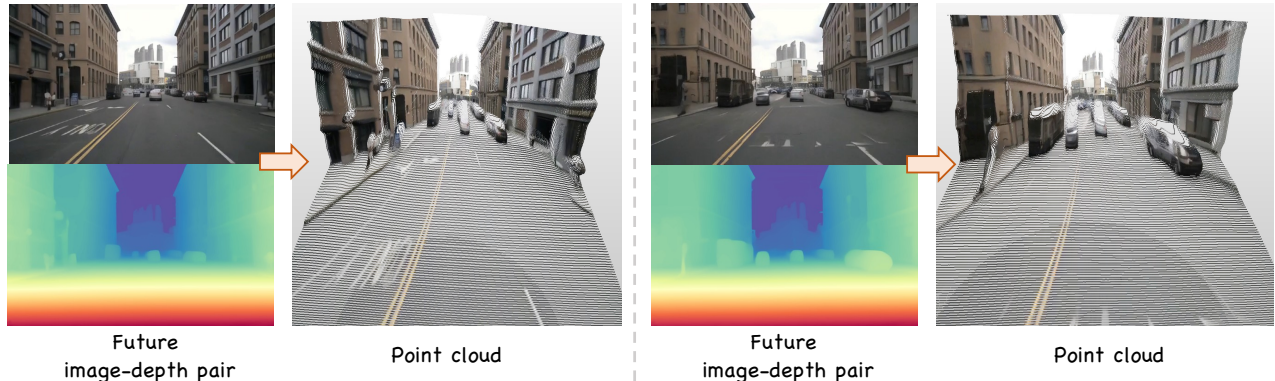


Figure 6. 4D point cloud generated from the predicted future image-depth pairs. It indicates the potential of our method to construct the 4D world model.

Table 5. Ablation study of the proposed Multi-scale Latent Interaction (MLI) mechanism.

(a) The effectiveness of different multi-scale interactions.					(b) The effectiveness of inside and outside feedback.					(c) The influence of different feedback layers.					
Used scale	Generation		Perception		Inside	Outside	Generation		Perception		Setting	Generation		Perception	
	FID ↓	FVD ↓	AbsRel ↓	δ_1 ↑			FID ↓	FVD ↓	AbsRel ↓	δ_1 ↑		FID ↓	FVD ↓	AbsRel ↓	δ_1 ↑
1	12.9	114.4	9.677	91.1	-	-	13.3	123.3	9.034	91.5	Direct add	223.2	2474.6	53.177	49.9
$1, \frac{1}{2}, \frac{1}{4}$	12.6	106.9	9.277	91.4	✓	-	12.2	110.1	9.034	91.6	Random-conv	51.2	615.1	26.262	61.7
$1, \frac{1}{2}, \frac{1}{4}, \frac{1}{8}$	11.8	99.9	8.936	91.4	-	✓	13.5	119.0	9.100	91.4	Zero-conv	11.8	99.9	8.936	91.4

scheme, which unifies representations within a shared latent space via the shared VAE. A natural way for depth estimation is to adopt a conventional depth decoder, i.e., several simple convolutional layers. However, as shown in Tab. 4, while the conventional decoder can transform latent representations into depth, our DLS significantly improves both generation (FVD: 99.9 vs. 121.1) and perception (AbsRel: 8.936 vs. 11.874) performance. These results confirm that a shared pre-trained VAE decoder enforces high consistency between future image and depth predictions.

The effectiveness of multi-scale interactions in MLI mechanism. Our MLI mechanism is designed to facilitate cross-space refinement and bidirectional interaction between image and depth representations. As shown in Tab. 5a, compared to using only one scale, introducing multi-scale feedback significantly improves both future generation and perception performance. These results confirm that multi-scale interactions play a crucial role in aligning spatial structures across modalities, improving the overall quality of future predictions.

The effectiveness of inside and outside feedback. In our MLI, we adopt two different feedback types, including inside feedback in UNet and outside after UNet (refer to Fig. 4). Specifically, as shown in Tab. 5b, adding inside feedback reduces FVD from 123.3 to 110.1, indicating its crucial role, and outside feedback also provides reasonable improvements for the generation task. When both feedback

mechanisms are combined, FVD drops significantly to 99.9, and AbsRel drops to 8.936. These results validate that the joint inside and outside feedback not only benefits the future generation but also strengthens future perception.

The impact of different feedback types. We finally discuss the impact of different feedback types. As shown in Tab. 5c, direct addition leads to severe performance degradation across all metrics, indicating that naively merging features disrupt the latent representations. Using a randomly initialized convolution mitigates this issue but still results in high FID (51.2) and FVD (615.1), as the uncontrolled transformation introduces instability in early training. In contrast, our zero-initialized convolution achieves the best performance, as depth and image spaces have an inherent gap. By initializing the convolution weights to zero, we gradually learn the optimal transformation between the two spaces, ensuring a smooth adaptation process.

5.6. Qualitative Results

We present qualitative comparisons in Fig. 5, highlighting the advantages of our approach. Compared to specialized models, our method generates more realistic future frames while achieving accurate depth estimation. This demonstrates the effectiveness of unifying the future generation and perception within a single framework. Besides, our method ensures strong alignment between generated images and depth maps, preserving geometric details and structural

integrity across future predictions.

Besides, we also demonstrate the potential of our **UniFuture** for generating the 4D point cloud, enabling 4D world dynamic modeling. As illustrated in Fig. 6, the output future image-depth pairs are used to reconstruct dynamic environments over time and finally obtain 4D representation with point cloud. More qualitative analyses are provided *in the Appendix*, e.g., controllable evolution, zero-shot.

6. Conclusion

We propose **UniFuture**, a unified world model that integrates future scene generation and depth-aware perception. Through Dual-Latent Sharing (DLS) and Multi-scale Latent Interaction (MLI), our method enables effective cross-modal representation learning and bidirectional refinement, enhancing structural consistency. Experiments show that our method achieves state-of-the-art performance, producing high-consistency image-depth pairs with improved realism and geometric alignment. By unifying the future generation and perception, we offer a valuable alternative to world modeling for autonomous driving.

Limitation. While **UniFuture** focuses on integrating future scene generation and perception, it primarily captures geometric consistency without explicitly modeling semantic information. Extending the framework to incorporate high-level semantic understanding could further enhance scene reasoning.

References

- [1] Shariq Farooq Bhat, Ibraheem Alhashim, and Peter Wonka. Adabins: Depth estimation using adaptive bins. In *Proc. of IEEE Intl. Conf. on Computer Vision and Pattern Recognition*, pages 4009–4018, 2021. 3
- [2] Shariq Farooq Bhat, Reiner Birkel, Diana Wofk, Peter Wonka, and Matthias Müller. Zoedepth: Zero-shot transfer by combining relative and metric depth. *arXiv preprint arXiv:2302.12288*, 2023. 3
- [3] Andreas Blattmann, Tim Dockhorn, Sumith Kulal, Daniel Mendelevitch, Maciej Kilian, Dominik Lorenz, Yam Levi, Zion English, Vikram Voleti, Adam Letts, et al. Stable video diffusion: Scaling latent video diffusion models to large datasets. *arXiv preprint arXiv:2311.15127*, 2023. 3
- [4] Holger Caesar, Varun Bankiti, Alex H Lang, Sourabh Vora, Venice Erin Liong, Qiang Xu, Anush Krishnan, Yu Pan, Giancarlo Baldan, and Oscar Beijbom. nuscenes: A multi-modal dataset for autonomous driving. In *Proc. of IEEE Intl. Conf. on Computer Vision and Pattern Recognition*, pages 11621–11631, 2020. 5
- [5] Yuntao Chen, Yuqi Wang, and Zhaoxiang Zhang. Driving-gpt: Unifying driving world modeling and planning with multi-modal autoregressive transformers. *arXiv preprint arXiv:2412.18607*, 2024. 2, 3
- [6] Yiquan Duan, Xianda Guo, and Zheng Zhu. Diffusiondepth: Diffusion denoising approach for monocular depth estimation. In *Proc. of European Conference on Computer Vision*, pages 432–449. Springer, 2024. 2
- [7] Huan Fu, Mingming Gong, Chaohui Wang, Kayhan Batmanghelich, and Dacheng Tao. Deep ordinal regression network for monocular depth estimation. In *Proc. of IEEE Intl. Conf. on Computer Vision and Pattern Recognition*, pages 2002–2011, 2018. 3
- [8] Shenyuan Gao, Jiazhi Yang, Li Chen, Kashyap Chitta, Yihang Qiu, Andreas Geiger, Jun Zhang, and Hongyang Li. Vista: A generalizable driving world model with high fidelity and versatile controllability. In *Proc. of Advances in Neural Information Processing Systems*, pages 91560–91596, 2024. 1, 2, 3, 5, 6, 7, 13, 15, 16
- [9] Clément Godard, Oisín Mac Aodha, and Gabriel J Brostow. Unsupervised monocular depth estimation with left-right consistency. In *Proc. of IEEE Intl. Conf. on Computer Vision and Pattern Recognition*, pages 270–279, 2017. 3
- [10] Yanchen Guan, Haicheng Liao, Zhenning Li, Jia Hu, Runze Yuan, Yunjian Li, Guohui Zhang, and Chengzhong Xu. World models for autonomous driving: An initial survey. *IEEE Transactions on Pattern Analysis and Machine Intelligence*, 2024. 2
- [11] Xi Guo, Chenjing Ding, Haoxuan Dou, Xin Zhang, Weixuan Tang, and Wei Wu. Infinitydrive: Breaking time limits in driving world models. *arXiv preprint arXiv:2412.01522*, 2024. 2, 3
- [12] David Ha and Jürgen Schmidhuber. World models. In *Proc. of Advances in Neural Information Processing Systems*, 2018. 2
- [13] Mariam Hassan, Sebastian Stapf, Ahmad Rahimi, Pedro Rezende, Yasaman Haghghi, David Brüggemann, Isinsu Katircioglu, Lin Zhang, Xiaoran Chen, Suman Saha, et al. Gem: A generalizable ego-vision multimodal world model for fine-grained ego-motion, object dynamics, and scene composition control. *arXiv preprint arXiv:2412.11198*, 2024. 3, 12
- [14] Jing He, Haodong Li, Wei Yin, Yixun Liang, Leheng Li, Kaiqiang Zhou, Hongbo Zhang, Bingbing Liu, and Yingcong Chen. Lotus: Diffusion-based visual foundation model for high-quality dense prediction. *arXiv preprint arXiv:2409.18124*, 2024. 3
- [15] Anthony Hu, Lloyd Russell, Hudson Yeo, Zak Murez, George Fedoseev, Alex Kendall, Jamie Shotton, and Gianluca Corrado. Gaia-1: A generative world model for autonomous driving. *arXiv preprint arXiv:2309.17080*, 2023. 2
- [16] Wenbo Hu, Xiangjun Gao, Xiaoyu Li, Sijie Zhao, Xiaodong Cun, Yong Zhang, Long Quan, and Ying Shan. Depthcrafter: Generating consistent long depth sequences for open-world videos. *arXiv preprint arXiv:2409.02095*, 2024. 3
- [17] Xiaotao Hu, Wei Yin, Mingkai Jia, Junyuan Deng, Xiaoyang Guo, Qian Zhang, Xiaoxiao Long, and Ping Tan. Driving-world: Constructingworld model for autonomous driving via video gpt. *arXiv preprint arXiv:2412.19505*, 2024. 3
- [18] Fan Jia, Weixin Mao, Yingfei Liu, Yucheng Zhao, Yuqing Wen, Chi Zhang, Xiangyu Zhang, and Tiancai Wang. Adriver-i: A general world model for autonomous driving. *arXiv preprint arXiv:2311.13549*, 2023. 2

- [19] Junpeng Jiang, Gangyi Hong, Lijun Zhou, Enhui Ma, Hengtong Hu, Xia Zhou, Jie Xiang, Fan Liu, Kaicheng Yu, Haiyang Sun, et al. Dive: Dit-based video generation with enhanced control. *arXiv preprint arXiv:2409.01595*, 2024. [2](#)
- [20] Bingxin Ke, Anton Obukhov, Shengyu Huang, Nando Metzger, Rodrigo Caye Daudt, and Konrad Schindler. Repurposing diffusion-based image generators for monocular depth estimation. In *Proc. of IEEE Intl. Conf. on Computer Vision and Pattern Recognition*, pages 9492–9502, 2024. [2](#), [3](#), [6](#), [7](#), [13](#), [16](#)
- [21] Seung Wook Kim, Jonah Philion, Antonio Torralba, and Sanja Fidler. Drivegan: Towards a controllable high-quality neural simulation. In *Proc. of IEEE Intl. Conf. on Computer Vision and Pattern Recognition*, pages 5820–5829, 2021. [2](#), [6](#)
- [22] Qifeng Li, Xiaosong Jia, Shaobo Wang, and Junchi Yan. Think2drive: Efficient reinforcement learning by thinking with latent world model for autonomous driving (in carla-v2). In *Proc. of European Conference on Computer Vision*, pages 142–158. Springer, 2024. [1](#)
- [23] Xiaofan Li, Yifu Zhang, and Xiaoqing Ye. Drivingdiffusion: Layout-guided multi-view driving scenarios video generation with latent diffusion model. In *Proc. of European Conference on Computer Vision*, pages 469–485. Springer, 2024. [1](#), [2](#), [6](#)
- [24] Jiachen Lu, Ze Huang, Zeyu Yang, Jiahui Zhang, and Li Zhang. Wovogen: World volume-aware diffusion for controllable multi-camera driving scene generation. In *Proc. of European Conference on Computer Vision*, pages 329–345. Springer, 2024. [2](#), [6](#)
- [25] Luigi Piccinelli, Yung-Hsu Yang, Christos Sakaridis, Mattia Segu, Siyuan Li, Luc Van Gool, and Fisher Yu. Unidepth: Universal monocular metric depth estimation. In *Proc. of IEEE Intl. Conf. on Computer Vision and Pattern Recognition*, pages 10106–10116, 2024. [2](#)
- [26] Uchiha Rajapaksha, Ferdous Sohel, Hamid Laga, Dean Diepeveen, and Mohammed Bennamoun. Deep learning-based depth estimation methods from monocular image and videos: A comprehensive survey. *ACM Computing Surveys*, 56(12):1–51, 2024. [3](#)
- [27] René Ranftl, Katrin Lasinger, David Hafner, Konrad Schindler, and Vladlen Koltun. Towards robust monocular depth estimation: Mixing datasets for zero-shot cross-dataset transfer. *IEEE Transactions on Pattern Analysis and Machine Intelligence*, 44(3):1623–1637, 2020. [3](#), [5](#)
- [28] Jeff Rasley, Samyam Rajbhandari, Olatunji Ruwase, and Yuxiong He. Deepspeed: System optimizations enable training deep learning models with over 100 billion parameters. In *Proc. of ACM SIGKDD*, pages 3505–3506, 2020. [6](#)
- [29] Robin Rombach, Andreas Blattmann, Dominik Lorenz, Patrick Esser, and Björn Ommer. High-resolution image synthesis with latent diffusion models. In *Proc. of IEEE Intl. Conf. on Computer Vision and Pattern Recognition*, pages 10684–10695, 2022. [3](#)
- [30] Minsoo Song, Seokjae Lim, and Wonjun Kim. Monocular depth estimation using laplacian pyramid-based depth residuals. *IEEE Transactions on Pattern Analysis and Machine Intelligence*, 31(11):4381–4393, 2021. [3](#)
- [31] Ziyang Song, Zerong Wang, Bo Li, Hao Zhang, Ruijie Zhu, Li Liu, Peng-Tao Jiang, and Tianzhu Zhang. Depthmaster: Taming diffusion models for monocular depth estimation. *arXiv preprint arXiv:2501.02576*, 2025. [3](#)
- [32] Sifan Tu, Xin Zhou, Dingkan Liang, Xingyu Jiang, Yumeng Zhang, Xiaofan Li, and Xiang Bai. The role of world models in shaping autonomous driving: A comprehensive survey. *arXiv preprint arXiv:2502.10498*, 2025. [1](#)
- [33] Xiaofeng Wang, Zheng Zhu, Guan Huang, Xinze Chen, Jiagang Zhu, and Jiwen Lu. Drivedreamer: Towards real-world-drive world models for autonomous driving. In *Proc. of European Conference on Computer Vision*, pages 55–72. Springer, 2024. [1](#), [2](#), [6](#)
- [34] Yuqi Wang, Jiawei He, Lue Fan, Hongxin Li, Yuntao Chen, and Zhaoxiang Zhang. Driving into the future: Multiview visual forecasting and planning with world model for autonomous driving. In *Proc. of IEEE Intl. Conf. on Computer Vision and Pattern Recognition*, pages 14749–14759, 2024. [2](#)
- [35] Yuqi Wang, Jiawei He, Lue Fan, Hongxin Li, Yuntao Chen, and Zhaoxiang Zhang. Driving into the future: Multiview visual forecasting and planning with world model for autonomous driving. In *Proc. of IEEE Intl. Conf. on Computer Vision and Pattern Recognition*, pages 14749–14759, 2024. [1](#), [3](#), [6](#)
- [36] Yuqing Wen, Yucheng Zhao, Yingfei Liu, Fan Jia, Yanhui Wang, Chong Luo, Chi Zhang, Tiancai Wang, Xiaoyan Sun, and Xiangyu Zhang. Panacea: Panoramic and controllable video generation for autonomous driving. In *Proc. of IEEE Intl. Conf. on Computer Vision and Pattern Recognition*, pages 6902–6912, 2024. [1](#), [2](#), [6](#)
- [37] Yuqing Wen, Yucheng Zhao, Yingfei Liu, Fan Jia, Yanhui Wang, Chong Luo, Chi Zhang, Tiancai Wang, Xiaoyan Sun, and Xiangyu Zhang. Panacea: Panoramic and controllable video generation for autonomous driving. In *Proc. of IEEE Intl. Conf. on Computer Vision and Pattern Recognition*, pages 6902–6912, 2024. [2](#)
- [38] Wei Wu, Xi Guo, Weixuan Tang, Tingxuan Huang, Chiyu Wang, Dongyue Chen, and Chenjing Ding. Drivescape: Towards high-resolution controllable multi-view driving video generation. *arXiv preprint arXiv:2409.05463*, 2024. [3](#)
- [39] Zehuan Wu, Jingcheng Ni, Xiaodong Wang, Yuxin Guo, Rui Chen, Lewei Lu, Jifeng Dai, and Yuwen Xiong. Holodrive: Holistic 2d-3d multi-modal street scene generation for autonomous driving. *arXiv preprint arXiv:2412.01407*, 2024. [1](#)
- [40] Jialei Xu, Yuanchao Bai, Xianming Liu, Junjun Jiang, and Xiangyang Ji. Weakly-supervised monocular depth estimation with resolution-mismatched data. *arXiv preprint arXiv:2109.11573*, 2021. [2](#)
- [41] Jiazhi Yang, Shenyuan Gao, Yihang Qiu, Li Chen, Tianyu Li, Bo Dai, Kashyap Chitta, Penghao Wu, Jia Zeng, Ping Luo, Jun Zhang, Andreas Geiger, Yu Qiao, and Hongyang Li. Generalized predictive model for autonomous driving. In *Proc. of IEEE Intl. Conf. on Computer Vision and Pattern Recognition*, 2024. [1](#), [2](#), [3](#), [6](#)
- [42] Lihe Yang, Bingyi Kang, Zilong Huang, Xiaogang Xu, Jiashi Feng, and Hengshuang Zhao. Depth anything: Un-

- leashing the power of large-scale unlabeled data. In *Proc. of IEEE Intl. Conf. on Computer Vision and Pattern Recognition*, pages 10371–10381, 2024. [2](#), [3](#)
- [43] Lihe Yang, Bingyi Kang, Zilong Huang, Zhen Zhao, Xiaogang Xu, Jiashi Feng, and Hengshuang Zhao. Depth anything v2. In *Proc. of Advances in Neural Information Processing Systems*, pages 21875–21911, 2024. [3](#), [5](#), [12](#)
- [44] Zhuoran Yang, Xi Guo, Chenjing Ding, Chiyu Wang, and Wei Wu. Physical informed driving world model. *arXiv preprint arXiv:2412.08410*, 2024. [3](#)
- [45] Weihao Yuan, Xiaodong Gu, Zuozhuo Dai, Siyu Zhu, and Ping Tan. Neural window fully-connected crfs for monocular depth estimation. In *Proc. of IEEE Intl. Conf. on Computer Vision and Pattern Recognition*, pages 3916–3925, 2022. [3](#)
- [46] Chi Zhang, Wei Yin, Billzb Wang, Gang Yu, Bin Fu, and Chunhua Shen. Hierarchical normalization for robust monocular depth estimation. In *Proc. of Advances in Neural Information Processing Systems*, pages 14128–14139, 2022. [3](#)
- [47] Guosheng Zhao, Xiaofeng Wang, Zheng Zhu, Xinze Chen, Guan Huang, Xiaoyi Bao, and Xingang Wang. Drivedreamer-2: Llm-enhanced world models for diverse driving video generation. *arXiv preprint arXiv:2403.06845*, 2024. [2](#)
- [48] Xin Zhou, Dingkan Liang, Sifan Tu, Xiwu Chen, Yikang Ding, Dingyuan Zhang, Feiyang Tan, Hengshuang Zhao, and Xiang Bai. Hermes: A unified self-driving world model for simultaneous 3d scene understanding and generation. *arXiv preprint arXiv:2501.14729*, 2025. [1](#)

A. The Comparison with Concurrent Work

As discussed in Sec.2.1 of the main paper, during the preparation of this manuscript, a concurrent work, GEM [13], emerged in Arxiv. To evaluate the effectiveness of our approach, we conduct a comparison with GEM, as shown in Tab. A1.

For the generation task, our method achieves highly competitive performance. Unlike GEM, which concatenates noisy RGB images with depth latent features and processes them jointly within the UNet, our approach explicitly decouples image and depth spaces while enabling bidirectional interaction. This strategic separation prevents the SVD model from having to compromise between image and depth modeling capacity. As a result, our method preserves the original image generation quality while seamlessly incorporating depth priors to enhance consistency.

For the perception task, our method also demonstrates superior performance. Since GEM jointly denoises image and depth without explicitly addressing their intrinsic domain gap, it inherently limits the structural coherence of the estimated depth. In contrast, our explicit decoupling strategy and bidirectional feedback enable more structured depth reasoning while maintaining generative fidelity. The results in Tab. A1 further validate that our design leads to both better depth perception and enhanced generative consistency.

B. Details of Depth Evaluation Settings

As mentioned in the main paper, to evaluate the consistency between the predicted future depth and the future scene, we utilize DepthAnythingV2 [43] to process the predicted future scene as pseudo-depth labels. Since some pixels have infinite depth values (e.g., sky) and should be excluded from a reasonable evaluation, we need to pre-process the depth before calculating the depth metrics. Thus, in this section, we provide more details about the depth evaluation settings of UniFuture, shown in Algorithm 1.

Because DepthAnythingV2 outputs inverse relative depth values, we need to transform these values to regular depths first. Then, following the conventional practices, we filter out invalid pixels (i.e., sky pixels with infinite depth) and align the scale of predicted and target relative depth for reasonable comparison. To do so, we ignore pixels with depth values greater than a certain threshold (we set 1000), as we found this can almost remove all sky pixels. To mitigate the impact of outliers, we further filter out pixels beyond the 98% percentile of predicted depth, followed by the least squares estimation for alignment. Finally, we turn to specific metrics (i.e., AbsRel and δ accuracy) to evaluate the geometry modeling ability of UniFuture.

Table A1. Comparison of our method with concurrent GEM.

Method	Generation		Perception			
	FID ↓	FVD ↓	AbsRel ↓	δ_1 ↑	δ_2 ↑	δ_3 ↑
GEM [13]	10.5	158.5	17.0	79.0	-	-
UniFuture	11.8	99.9	8.936	91.4	97.6	98.9

Algorithm 1 Depth evaluation

```
DEPTH_EVAL_METRICS = [
    abs_rel,
    delta1,
    delta2,
    delta3,
]

def eval_depth(output, target, thresh=1000):
    """
    Args:
        output: inversed depth prediction from UniFuture
        target: inversed depth target
        thresh: the threshold for invalid pixel exclusion
    """
    # 1. transform inversed depth to depth
    actual_output = 1. / output
    actual_target = 1. / target

    # 2. filter sky
    valid_mask = actual_target < thresh
    actual_output[~valid_mask] = 0
    actual_target[~valid_mask] = 0

    # 3. filter outliers
    h_th = torch.quantile(actual_output, 0.98)
    valid_mask = valid_mask & actual_output < h_th

    # 4. use least square to align the scale of output and target
    actual_output = align_depth_least_square(
        gt=actual_target,
        pred=actual_output,
        valid_mask=valid_mask,
    )

    # 5. calculate metrics (AbsRel and delta)
    results_dict = dict()
    for met_func in DEPTH_EVAL_METRICS:
        _metric_name = met_func.__name__
        _metric = met_func(actual_output,
            actual_target, valid_mask)
        results_dict[_metric_name] = _metric
    return results_dict
```

C. Controllable Future Scene Evolution

A crucial characteristic of world models in autonomous driving is their ability to predict future scene evolution based on control signals. Only with this capability can the world model provide a realistic simulation environment, thereby supporting the development of end-to-end reinforcement learning models.

Thus, in this section, we present the results of UniFuture for controllable future scene evolution, shown in Fig. A1. Starting from the same condition frame, our method can generate different future scenes corresponding to given commands (e.g., go straight, turn right) with high-quality geometry outputs (i.e., depth). These results demonstrate the potential of our method to support downstream

tasks, showing the superiority of **UniFuture**.

D. Zero-Shot Qualitative Results

As shown in Fig. A2, we present zero-shot qualitative results comparing **UniFuture** with the baseline Vista [8] on the Waymo dataset. Our method successfully generates realistic future frames while simultaneously predicting accurate depth maps, demonstrating its ability to model both appearance and geometry in novel environments. In contrast, Vista, which focuses solely on image synthesis, lacks explicit geometric reasoning. The depth predictions produced by **UniFuture** exhibit strong structural consistency with the generated images. These results highlight our model’s capacity to generalize to unseen datasets while maintaining both temporal coherence and geometric fidelity.

E. Additional Qualitative Results

This section presents additional visualizations to highlight the effectiveness of our method, as shown in Fig. A3. Compared to Vista [8], which lacks depth awareness and produces structurally inconsistent predictions, and Marigold [20], which only estimates depth for a single frame, our UniFuture model generates both temporally stable images and geometrically consistent depth maps.

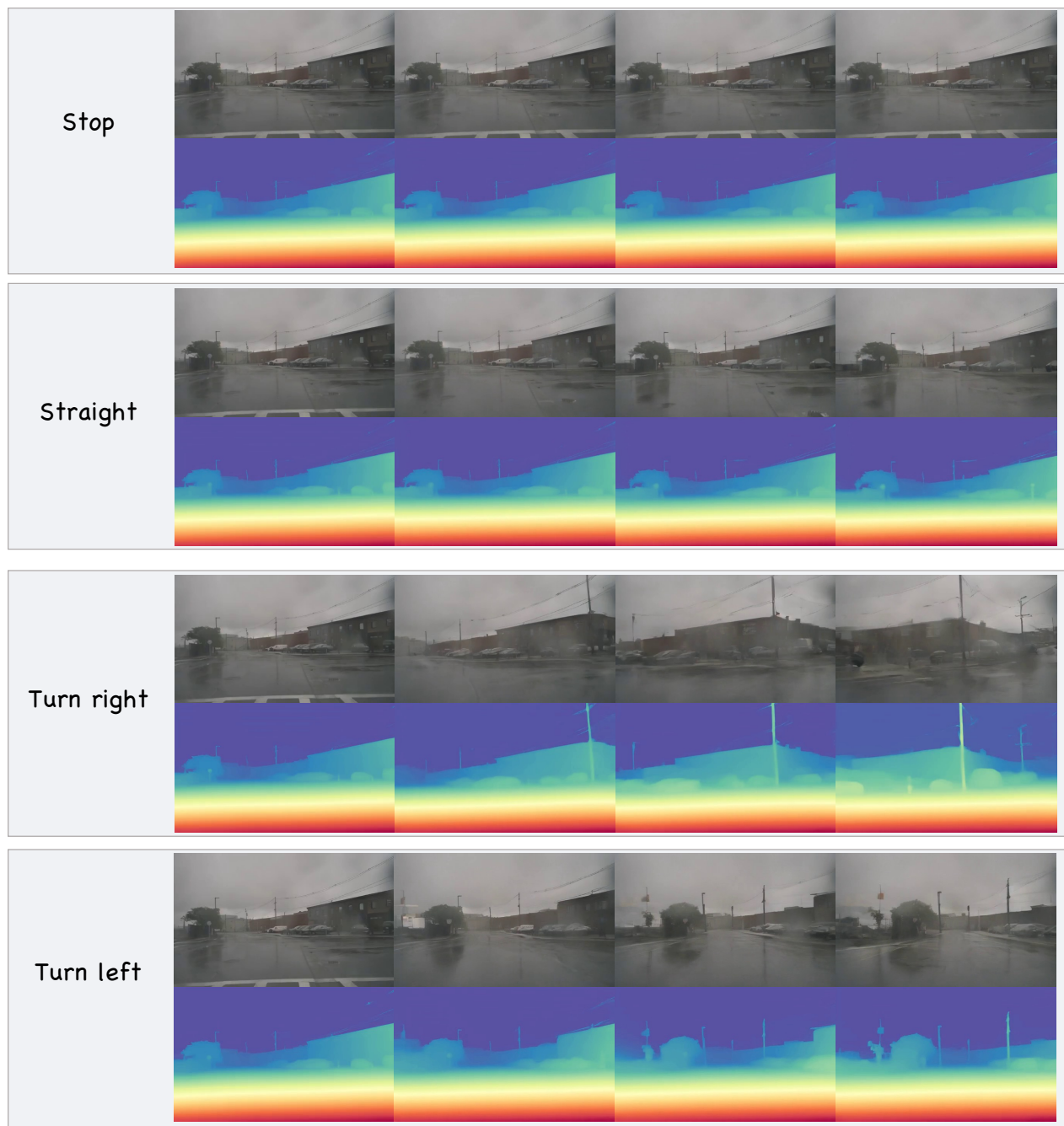


Figure A1. Controllable future scene evolution with **UniFuture**. Given the same starting frame, our method generates diverse future trajectories based on different control commands (e.g., stop, go straight, turn right, turn left) while maintaining high-quality geometric consistency.

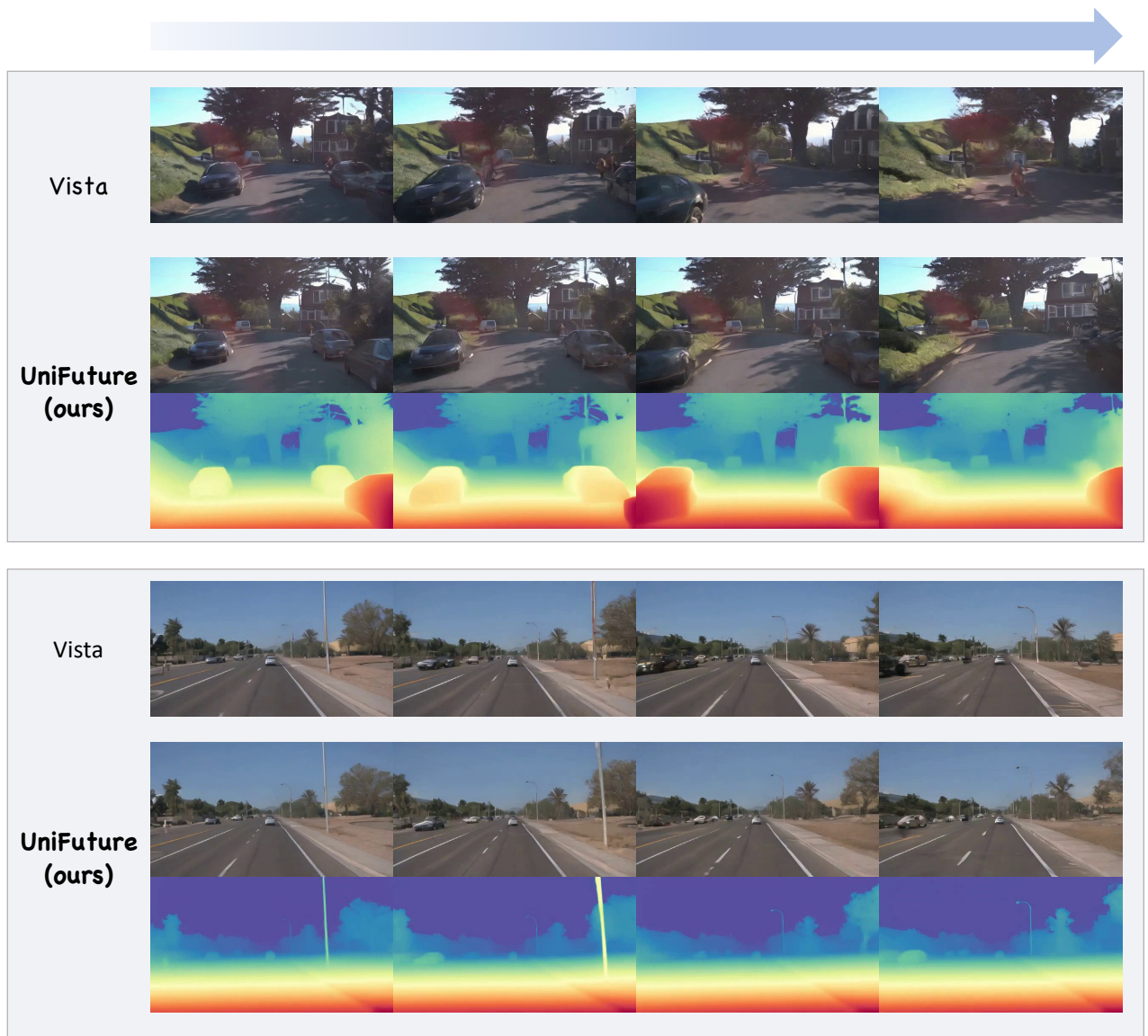


Figure A2. Zero-shot qualitative results on the Waymo dataset. We compare our UniFuture with the baseline Vista [8] on future frame prediction. Our model not only generates realistic future frames but also predicts corresponding depth maps, enabling a structured understanding of scene evolution. The results demonstrate our method’s ability to generalize to unseen data while maintaining geometric consistency.

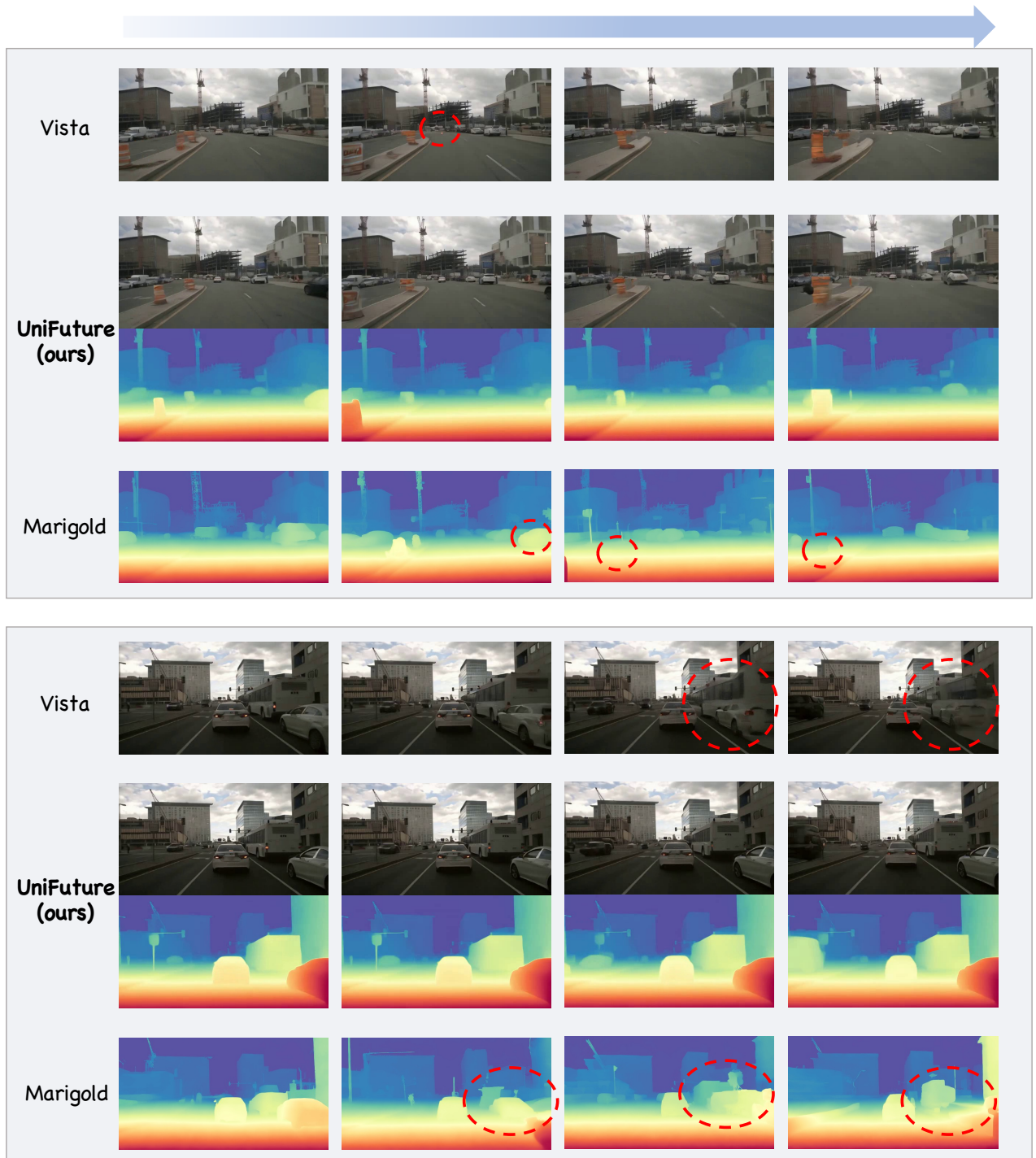


Figure A3. Qualitative comparisons between different models. The existing world model (Vista [8]) lacks depth awareness, leading to inaccurate scene understanding. Depth estimation models (Marigold [20]) fail to predict future depth, limiting their ability to capture scene evolution. In contrast, our **UniFuture** delivers more coherent future predictions, enhancing both generation and perception tasks.